(Received 4 December 2025, Accepted 13 January 2026, Scheduled 27 April 2026)

Design and Analysis of a Tri-Split-Ring Resonator Integrated Rectangular DRA with E-Shaped Feed for Enhanced C-Band Performance

Syamala Misala[1, *], Dwarapu Lakshmi Narayana[2], and Kanthamma Bokka[3]

[1] *Department of ECE, Lendi Institute of Engineering and Technology, Jonnada, Vizianagaram, India*
[2] *Department of ECE, Vignan's Institute of Engineering for Women, Visakhapatnam, India*
[3] *Department of ECE, Visakha Institute of Engineering and Technology, Visakhapatnam, India*

ABSTRACT: This paper presents a tri-split-ring resonator (TSRR) integrated with a rectangular dielectric resonator antenna (RDRA) using an E-shaped microstrip feed line. The RDRA, measuring $15 \times 14 \times 14\,\text{mm}^3$ and constructed on an FR4 substrate of $46 \times 46 \times 1.6\,\text{mm}^3$, features a gain of 10.9 dBi and a fractional bandwidth of 22.05% (5.85 GHz–7.3 GHz) with radiation efficiency over 82%. It supports fundamental modes TE_{111} at 6.12 GHz, along with lower- and higher-order modes $TE_{1\delta2}$ at 6.13 GHz, $TE_{3\delta3}$ at 6.14 GHz, and TE_{333} at 6.2 GHz. Simulated and measured results show close agreement across the operating band. The proposed antenna has several applications, including point-to-point microwave links (5.925 GHz–7.125 GHz), satellite communication in the C-band, and defense and military communication.

1. INTRODUCTION

In the current 5G wireless communications system, antennas are crucial. Seaquake communications call for compact, wideband, high-data-rate, and high-efficiency antennas. Dielectric-resonator antennas [1] are simpler and less expensive to fabricate tnan microstrip patch antennas (at higher frequencies). The best possible radiator in 1980, according to Long et al. [2], was a DRA rather than a microstrip patch or a dipole antenna. Dielectric Resonator Antennas (DRAs) [3] are attracting increased attention because of their alluring characteristics, such as negligible conduction losses, high gain, and radiation efficiency. DRA features several notable and appealing physical properties, including 3D construction flexibility, lightweight, cheap cost, ease of excitation, and increased performance in terms of gain and bandwidth (BW) [4]. According to a literature review, there are conventional methods that can be used to increase bandwidth and gain. These methods include conformal strips, parasitic strips, folded metallic patches, antenna offset wells, vertical strips, square spiral strips, complementary rectangular split-ring resonators (CRSRR), parasitic conducting strips, metamaterial low-profile stacked DRAs, and dual pairs of microstrip lines [5–16]. A rectangular DRA (RDRA) featuring a parasitic strip and a triangular ring-shaped aperture operates effectively in dual bands, achieving gains of 5.1 dBi and 5.25 dBi, making it appropriate for WiMAX and WLAN applications in the frequency ranges of 3.4–3.58 GHz and 5.1–5.9 GHz [17]. A hexagonal dielectric resonator with a square microstrip ring operates in triple bands, achieving 10 dB impedance bandwidths of 17.4%, 28.13%, and 2.97%, with respective gains of 5, 5.28, and 2.36 dBic [18]. A single-fed wideband DRA achieved a peak gain of 4.73 dBic by sequentially spinning four metallic plates [19]. An RDRA powered by an E-shaped parasitic patch [20] has a 10 dB impedance bandwidth of 21% at a frequency of 4.02 GHz and a gain of 6.5 dB. An RDRA with a unique conformal H-shaped metal strip [21] exhibits a 27.7% impedance bandwidth (3.67 GHz–4.73 GHz) and a gain of 6.8 dBi. A DRA array, featuring a rectangular dielectric resonator antenna array [22] and an air-bridgeless coplanar waveguide power divider, provides a wide response with a measured impedance bandwidth of 14.8%. An RDRA [23] featuring a T-shaped feeding strip and parasitic patch, stimulated by a coaxial probe, achieves a 10 dB impedance bandwidth of 17.3% and a gain of 6.32 dBi, suitable for WiMAX, satellite, and Sub-6 5 GHz band communications. This study describes a method for energizing a dielectric resonator [24] using a metallic circular patch antenna in the millimeter wave frequency range, which includes a rectangular slot and an across-slot aperture. The gain of the single-element non-metallic dielectric resonator antenna is increased from 6.38 dB to 8.04 dB. An RDRA with a patch strip activated by a coaxial probe achieved a 10 dB impedance bandwidth of 48% and a gain of above 6 dBi [25]. Illahi et al. proposed an RDRA [26] featuring a conformal strip design, yielding an impedance bandwidth of 17% between 4.05 GHz and 4.81 GHz, with a gain of 6.2 dBi, suitable for 5G NR Sub-6 GHz applications. Additionally, an RDRA [27] utilizing F-shaped metal strips achieves impedance-matching bandwidths of 35.4%, 1.74%, and 1.85%, with peak gains of 6.8 dBic, 7.6 dBic, and 8.5 dBic. A hybrid RDRA presents a modified microstrip octagonal feed [28] and a plus-shaped slotted ground plane, achieving a 5.5 dBi gain suitable for WLAN,

* Corresponding author: Syamala Misala (msyamala869@gmail.com).

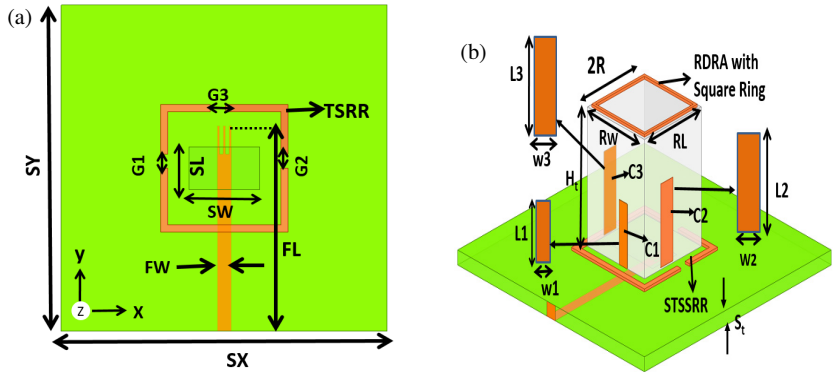

FIGURE 1. The geometric view of TSRR. (a) TSRR top view without RDRA. (b) Isometric view of RDRA with conformal strips C1, C2, C3, and square ring.

TABLE 1. Parameters and dimensions (mm) of the proposed antenna tri-split-ring resonator.

Parameter	Dimension	Parameter	Dimension	Parameter	Dimension	Parameter	Dimension
H_t	15	S_t	1.6	W_S	3	$W2$	3
$2R$	14	FW	29	$L1$	7	$W3$	3
SW	10	FL	2	$W1$	2	$G1$	2.2
SL	6	$TL = TW$	16	$L2$	8	$G2$	2.2
$Sx = Sy$	46	$RL = RW$	13	$L3$	8	$G3$	2.2

WIMAX, and WAIC applications. Additionally, an RDRA with a ring slot [29] exhibits triple-band radiation efficiencies of 90%, 87%, and 84%, alongside 10 dB impedance bandwidths of 3.4%, 7.7%, and 1.9%, with corresponding gains of 7.3 dBi, 6.5 dBi, and 5.8 dBi. A stacked rectangular dielectric resonator antenna incorporating a surface mounted short rectangle (SMSR) [30] and an E-shaped microstrip feed achieved a 10 dB impedance bandwidth of 21.5% and a gain of 10.5 dB, making it suitable for wireless communication applications. The rectangular DR in [31] is powered by a quarter-wave transformer and has an extended rectangle-shaped feed line with split-ring resonators (SRRs) for multiband wireless applications. A cylindrical dielectric resonator antenna (CDRA) [32] array featuring a quarter-wavelength transformer and power divider network exhibits impedance bandwidths of 18%, 17%, and 22% across three bands, achieving peak gains of 2.43 dBi, 7.72 dBi, and 8.39 dBi, making it suitable for GPS navigation, Wi-Fi, Bluetooth, and satellite applications. A triple-band CDRA array [33] with bandwidths of 1.14 GHz, 0.26 GHz, and 0.22 GHz achieved gains of 8.01 dBi, 7.4 dBi, and 9 dBi for WiFi, wireless LAN, and satellite applications.

This design combines TSRR, square ring loading, and multi-side conformal strip excitation to produce a broad fractional bandwidth of 22.05% width and excellent impedance matching (-47 dB). It may be employed in single parasitic strips, stacked structures, or simple ring slots. The suggested antenna achieves a better gain of 10.9 dBi in a small $15 \times 14 \times 14$ mm^3 DRA configuration, surpassing most documented single-element RDRA designs in the comparison table. A key contribution is the systematic excitation and transformation of modes TE_{111} to higher order TE_{333} from the fundamental to higher-order modes through conformal strips and square ring loading, enabling bandwidth and gain enhancement. Therefore, the work is more novel than exciting designs because it uniquely integrates metamaterial-inspired TSRR loading with controlled higher-order mode excitation to simultaneously improve feeding efficiency, bandwidth, and gain in the C-band.

2. DESIGN AND CONFIGURATION OF ANTENNA

The proposed tri-split-ring resonator (TSRR) integrates a novel RDRA excited by a square ring with conformal strips, as illustrated in two stages in this section. Fig. 1(a) shows the TSRR without RDRA. In the first stage, an E-shaped microstrip feed line is placed on the ground plane without RDRA. An isometric view of the RDRA integrated TSRR with conformal strips and a square ring on RDRA is shown in Fig. 1(b). The bandwidth enhancement is carried out by introducing the vertical conformal strip (C1) at the microstrip feed, the right conformal strip (C2), and the left conformal strip (C3) at an optimal location near the rectangular DRA. A square copper ring on the RDRA, along with three conformal strips and TSRR, enhances antenna impedance bandwidth, gain, and radiation efficiency while enabling higher-order modes through an economical excitation method. The RDRA is situated on an FR4 substrate with permittivity $\varepsilon_r = 4.4$, loss tangent $\tan\delta = 0.02$, and thickness $st = 1.6$ mm. Design parameters are detailed in Table 1, and the resonance frequency is determined using a specified equation [33]

$$f_{res} = \frac{397}{2\pi r}\left(C_O^R\right) \tag{1}$$

where $R = \frac{Width\,fDRA}{2}$ and $C_0^R = \frac{1.6+0.513K+1.392K^2-0.574K^3+0.88K^4}{\varepsilon_{dr}^{0.42}}$, $K = \frac{R}{2*H_t}$.

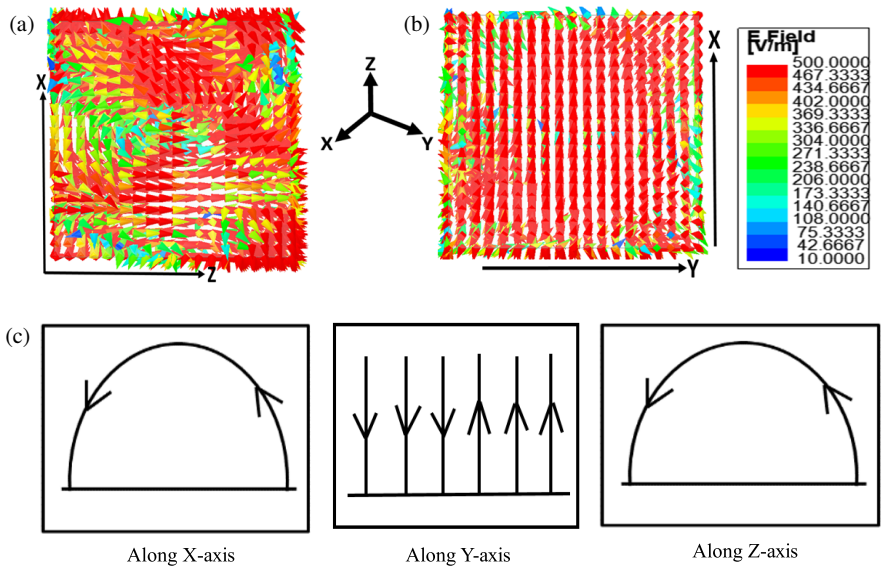

FIGURE 2. E-field distribution without conformal strips TSRR and RDRA of the antenna for the mode TE_{111}. (a) Y-Z plane phi $= 0^\circ$. (b) X-Z plane phi $= 0^\circ$ at 6.12 GHz. (c) Sketch of E-fields.

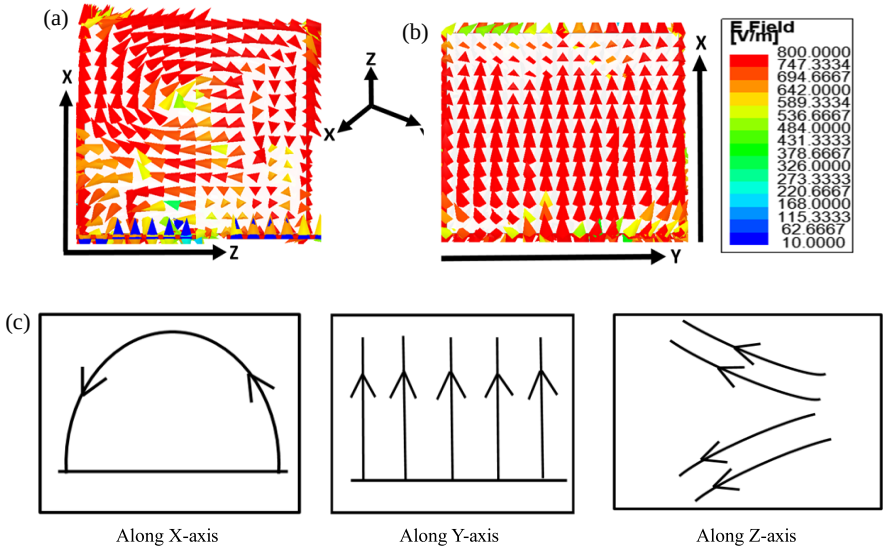

FIGURE 3. E-field distribution without conformal strips TSRR and RDRA of the antenna for the mode $TE_{1\delta 2}$. (a) X-Z plane Phi $= 0^\circ$. (b) X-Y plane Phi $= 0^\circ$ at 6.13 GHz. (c) A sketch of electric fields.

3. GENERATION OF HIGHER-ORDER MODES BY CONFORMAL STRIP EXCITATION CONFIGURATION-1

The rectangular dielectric resonance antenna (RDRA) is composed of alumina, offering a higher dielectric constant than the FR4 substrate, which restricts electromagnetic radiation. The E-shaped microstrip feed generates electric fields, seen in Figs. 2(a) and (b), which interact with the FR4 substrate and tri-split-ring resonator edges, resulting in standing waves with resonant mode patterns at 6.12 GHz and vector representation, as shown in Fig. 2(c) depicts the vector representation of the E-field. The electric field exhibits variations without conformal strips, following one-half cycle along the X, Y, and Z axes, characterized as the fundamental mode TE_{111}.

3.1. Configuration-2

A microstrip feed featuring an E-shaped design excites a rectangular dielectric resonator antenna. In Stage 2, a vertical conformal strip (C1) is added in front of the DRA and connected to the microstrip feed, enhancing coupling and matching. This setup facilitates energy transfer from the microstrip feed to C1, potentially altering field distributions and improving radiation or creating new resonant modes. The first harmonic (lower order mode) is excited at 6.13 GHz, as shown in Figs. 3(a) and (b), which represent the direction of the electric field, and Fig. 3(c), which shows the vector representation of the E-field. The electric field variation due to strip C1, with one half cycle along the X-axis, uniform along the Y-axis, and two half cycles along the Z-axis, identified as the $TE_{1\delta 2}$ mode.

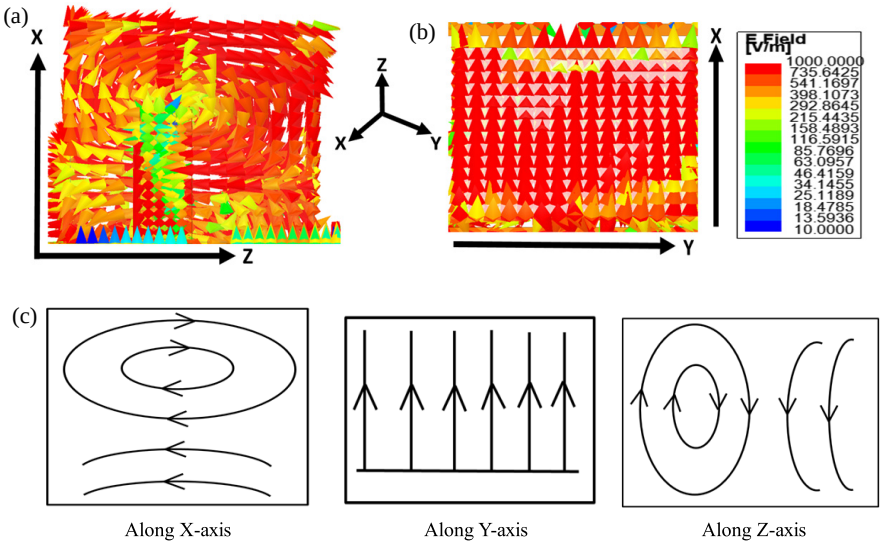

FIGURE 4. E-field distribution without conformal strips TSRR and RDRA of the antenna for the mode $TE_{3\delta 3}$. (a) X-Z plane Phi $= 0^\circ$. (b) X-Y plane Phi $= 0^\circ$ at 6.14 GHz. (c) A sketch of electric fields.

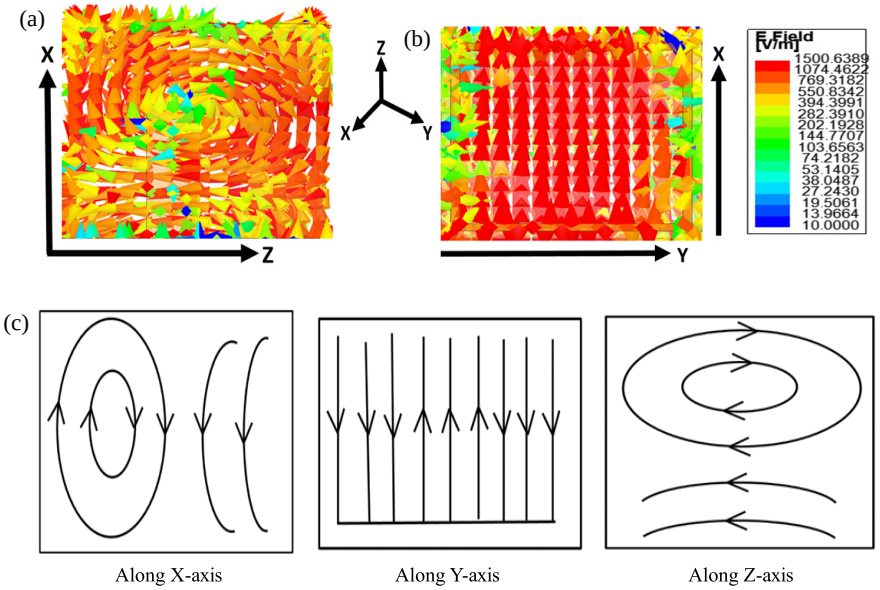

FIGURE 5. E-field distribution without conformal strips TSRR and RDRA of the antenna for the mode TE_{333}. (a) X-Z plane Phi $= 0^\circ$. (b) X-Y plane Phi $= 0^\circ$ at 6.2 GHz. (c) A sketch of electric fields.

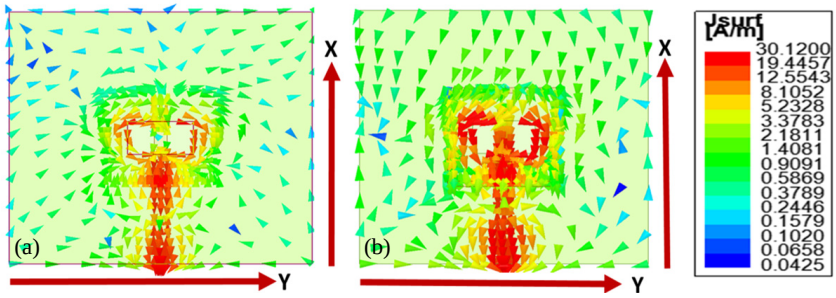

FIGURE 6. The proposed antenna's surface current variation of TSRR without rectangular DRA. (a) Top view (XY) Phi $= 0^\circ$. (b) Top view (XY) Phi $= 90^\circ$ at 6.2 GHz.

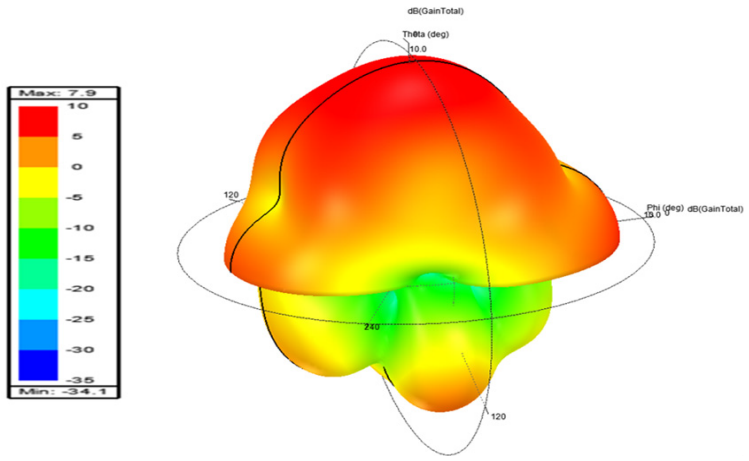

FIGURE 7. 3D far-field radiation pattern (directivity) of proposed antenna at 6.2 GHz.

TABLE 2. Evolution of antenna parameters comparison.

Stage	Position of the conformal strip	Description	fr (GHz)	%IMBW	S_{11} (dB)	Modes
Stage1	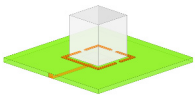	RDRA without conformal strips	6.12	4.39%	20.94	TE_{111}
Stage2	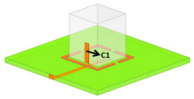	RDRA with conformal C1 and micro-strip feed(front side)	6.13	5.52%	23.28	$TE_{1\delta 2}$
Stage3	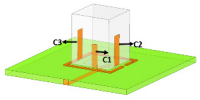	RDRA with Conformal stripsC1,C2 and C3 (front side, right side and left side)	6.14	12.86%	21.13	$TE_{3\delta 3}$
Stage4	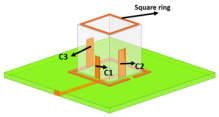	RDRA with Conformal strips C1, C2, C3 and Square ring (Proposed Design)	6.2	22.05%	47.4	TE_{333}

3.2. Configuration-3

This configuration involves placing conformal strips on the right (C2) and left (C3) sides of the RDRA, alongside the front vertical strip (C1). This arrangement effectively couples electromagnetic energy into the DRA, surpassing the energy coupling of probe-fed designs. The tri-split-ring resonator establishes localized fields, modifying the DRA's fundamental modes, the antenna's emission pattern, and impedance bandwidth. The second harmonic is excited at 6.14 GHz, as shown in Figs. 4(a) and (b), which represent the direction of the electric field, and Fig. 4(c), which shows the vector representation of the E-field. The electric field variations with three half-cycle changes along the X-axis, a uniform field along the Y-axis, and three half-cycle variations along the Z-axis for the $TE_{3\delta 3}$ mode.

3.3. Configuration-4

A square ring on the rectangular DRA modifies the E-field distribution through its electromagnetic modes. Conformal strips C1, C2, and C3 enhance energy within the ring, creating complex field patterns that improve RDRA performance by increasing impedance bandwidth and gain. In stage 4, these elements enhance higher-order modes at 6.2 GHz, generating stronger electric fields in the DRA, in particular the TE_{333} mode, as shown in Figs. 5(a), (b), which represent the direction of the electric field, and Fig. 5(c), which shows the vector representa-

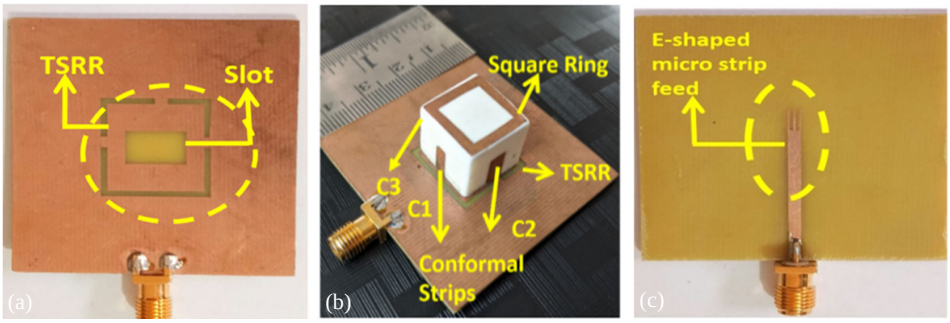

FIGURE 8. Prototype of the fabricated antenna. (a) Top view w/o RDRA. (b) Isometric view with DRA. (c) Bottom view.

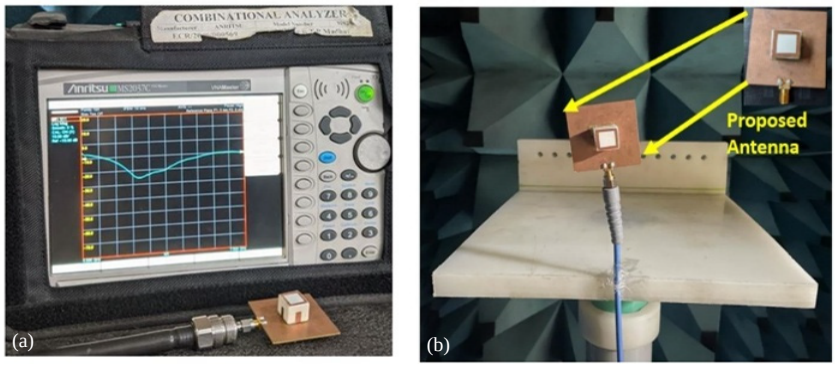

FIGURE 9. Measurement setup for (a) reflection coefficient, (b) gain and 2D radiation pattern.

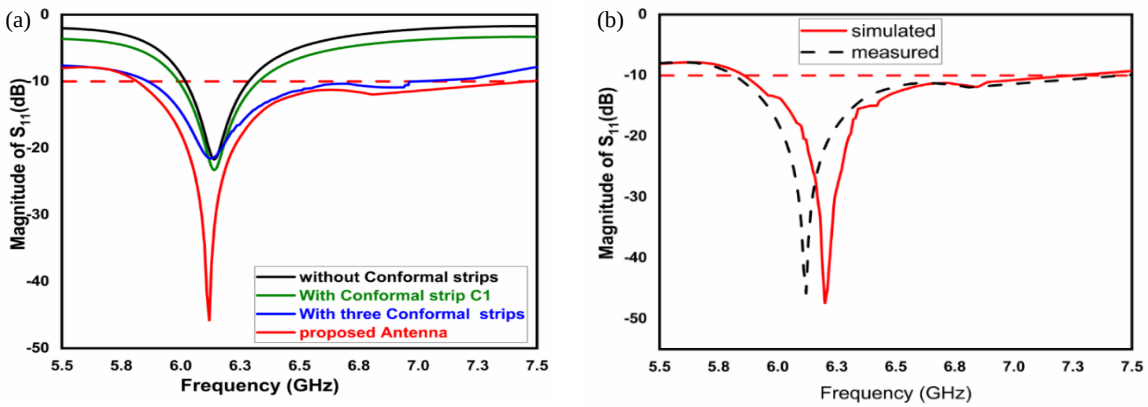

FIGURE 10. (a) Evolution of simulated reflection coefficient. (b) Comparison of simulated and measured reflection coefficients of the proposed antenna.

tion of the E-field. The positions of the conformal strip without and with conformal strips and the square ring of an antenna's parameters are compared as shown in Table 2.

Figure 6 depicts the surface current fluctuations of the proposed antenna, with top views at Phi $= 0°$ and $90°$, revealing that the current is mostly channelled toward an E-shaped microstrip feed. Due to fringing effects, the slots' corners and edges have greater current densities, especially at 6.2 GHz. Furthermore, Fig. 7 shows the antenna's three-dimensional far-field emission pattern and a maximum directivity of 7.9 dB at the same frequency.

4. RESULTS AND DISCUSSIONS

The fabricated prototype of the proposed antenna is shown in Fig. 8. The measurement setup depicted in Fig. 9(a) contains an Anritsu vector network analyzer (Model No. VNA MS2037C) for S_{11} analysis. The gain and 2D radiation patterns of the antenna are examined in an anechoic room using a typical waveguide horn antenna (1 GHz–40 GHz) and a Keysight signal generator (N5173 B), as shown in Fig. 9(b).

The simulated reflection coefficient analysis of the proposed antenna shows various impedance bandwidths: 4.39% without conformal strips, 5.52% with one strip, and 12.86% with three strips, and the corresponding return losses are 20.94 dB,

TABLE 3. Simulated and measured parameters of TSRR.

Antenna parameters	Simulated	Measured
Impedance bandwidth	5.85 GHz–7.3 GHz	5.82 GHz–7.3 GHz
Resonance frequency (f_r) GHz	6.2	6.15
%Impedance bandwidth	22.05	22.56
Return loss at f_r (dB)	47	46
E-plane Co-pol and X-pol (dB)	89.93°&80.46°	91.95°&81.48°
H-plane Co-pol and X-pol (dB)	46.62°&42.91°	47.92°&43.93°
Gain (dBi)	10.9	10.8

TABLE 4. Comparison of the proposed TSRR with RDRA performances with previous reported DRAs.

Ref. No /Year	Type of antenna	Size of DRA (mm^3)	Excitation technique	Band	f_r (GHz)	Mode	% Impedance BW	Gain (dBi)	RE(η) (%)
[25]/2021	RDRA	$26.1 \times 25.4 \times 14.3$	Patch strip	Triple	2.88, 5.2, 5.69	$TE^X_{\partial 11}$ $TE^X_{\partial 23}$ $TE^X_{\partial 23}$	46.24, 6.3, 2.5	6.25, 9.44, 9.3	NA
[26]/2022	RDRA	$26.1 \times 25.4 \times 14.3$	Uniquely shaped conformal strip	Single	4.53	$TE^X_{\partial 13}$ $TE^y_{1\partial 3}$	17	6.2	NA
[29]/2023	RDRA	$1.7 \times 3.8 \times 3.8$	Micro-strip feed	Triple	17.5, 23, 28.5	TE_{111} TE^X_{121} TE^Y_{211}	3.4, 7.7, 1.9	7.3, 6.8, 5.8	90, 87, 84
[30]/2024	RDRA	$15 \times 14 \times 14$	Micro-strip feed	Single	6.2	NA	20.1	10.7	91.4
[31]/2025	RDRA	$5 \times 20 \times 10$	Quarter wave transformer	Four	1.62, 3.03 4.4, 6.56	NA	9.2, 5 8.3, 5.6	1.5, 1.9 2.3, 2.1	NA
Present work	RDRA	$15 \times 14 \times 14$	Micro-strip feed with conformal strip	Single	6.2	TE_{111} $TE_{1\delta 2}$ $TE_{3\delta 3}$ TE_{333}	22.05	10.9	> 82

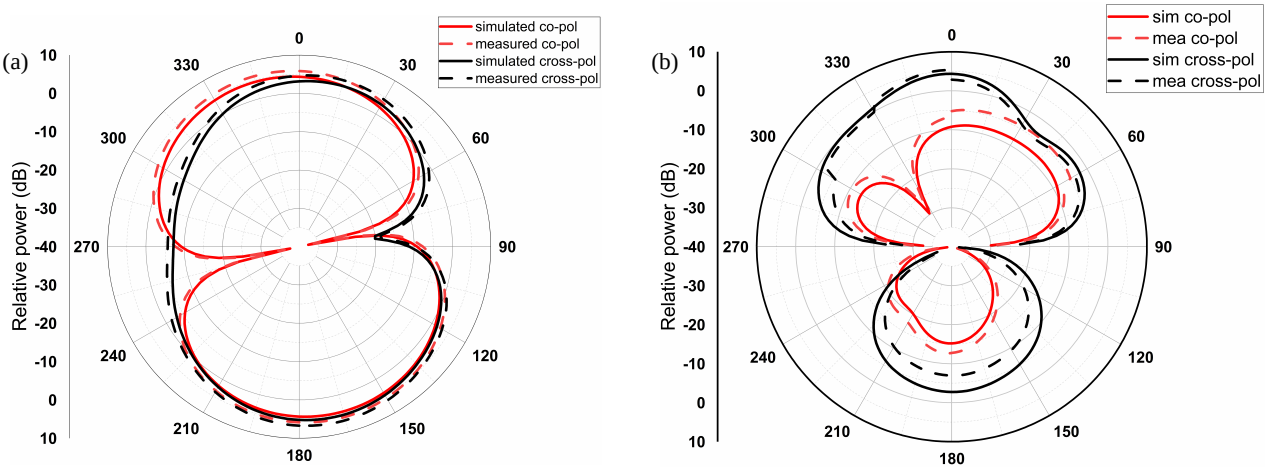

FIGURE 11. Radiation pattern at 6.2 GHz, (a) E-field, (b) H-field.

23.28 dB, and 21.13 dB respectively. The proposed antenna resonates at 6.2 GHz with a bandwidth of 22.05% and its return loss of 47.4 dB as shown in Fig. 10(a). The comparison between measured and simulated reflection coefficients is depicted in Fig. 10(b). The impedance bandwidths of simulation and measurement are 22.05% and 22.56%, respectively. The measured values reveal minor variances owing to manufacturing flaws and connection soldering. The measured and simulated radi-

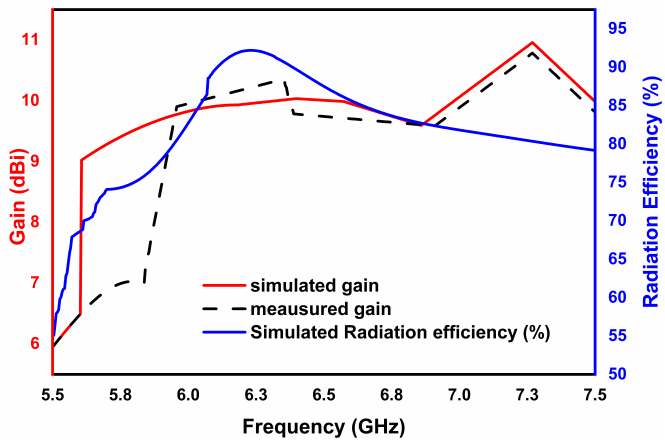

FIGURE 12. Comparison of simulated and measured gains and simulated radiation efficiency.

ation patterns for E-field and H-field at 6.2 GHz are shown in Fig. 11, in which co-polarization is approximately 10 dB difference with respect to cross-polarization for both fields. The measured E-plane and H-plane beamwidths are given by 91.95° and 47.92°, respectively, with simulated and observed 3 dB beamwidths being equivalent. The simulated and measured gains of the TSRR with RDRA in the bore sight direction ($\theta = 0°$ and $\varphi = 0°$) are depicted in Fig. 12. The maximum gain has been increased by activating the rectangle DRA with three conformal strips and a square ring. The suggested antenna has a simulated gain range of 9.4 dBi to 10.9 dBi in the frequency band (5.85 GHz–7.3 GHz), whereas the measured gain varies from 7.0 dBi to 10.8 dBi. The simulated radiation efficiency of the proposed antenna is more than 82% throughout teh operating band, as shown in Fig. 12. The simulated and measured parameters of the TSRR are mentioned in Table 3. Table 4 shows a comparison of previous research works to the proposed TSRR.

5. CONCLUSION

This paper introduces a tri-split-ring resonator (TSRR) integrated with a novel rectangular dielectric resonator antenna (RDRA) excited by a conformal strip. The design allows for mode conversion from fundamental TE_{111} modes to higher-order TE_{333} modes. The TSRR with RDRA operates in the frequency range of 5.85–7.3 GHz, offering a fractional impedance bandwidth of 22.56%, a gain of 10.8 dBi, a reflection coefficient of -46 dB, and a radiation efficiency exceeding 82%. The antenna features 3 dB beamwidths of 91.95° in the E plane and 47.92° in the H plane. Measured results match simulated predictions closely, indicating the design's suitability for C-band satellite communication applications.

ACKNOWLEDGEMENT

The authors would like to thank the Antenna laboratory team, KL University, Guntur, Andhra Pradesh, India, for their assistance in the fabrication and measurement of the antenna prototype model.

REFERENCES

[1] Petosa, A., A. Ittipiboon, Y. M. M. Antar, D. Roscoe, and M. Cuhaci, "Recent advances in dielectric-resonator antenna technology," *IEEE Antennas and Propagation Magazine*, Vol. 40, No. 3, 35–48, 1998.

[2] Long, S., M. McAllister, and L. Shen, "The resonant cylindrical dielectric cavity antenna," *IEEE Transactions on Antennas and Propagation*, Vol. 31, No. 3, 406–412, 1983.

[3] Divya, G., K. J. Babu, and R. Madhu, "A synoptic review on dielectric resonator antennas," *Microelectronics, Electromagnetics and Telecommunications: Proceedings of ICMEET 2017*, 185–196, 2018.

[4] Dash, S. K. K. and T. Khan, "Recent developments in bandwidth improvement of dielectric resonator antennas," *International Journal of RF and Microwave Computer-Aided Engineering*, Vol. 29, No. 6, e21701, 2019.

[5] Leung, K. W., "Conformal strip excitation of dielectric resonator antenna," *IEEE Transactions on Antennas and Propagation*, Vol. 48, No. 6, 961–967, 2000.

[6] Long, R. T., R. J. Dorris, S. A. Long, M. A. Khayat, and J. T. Williams, "Use of parasitic strip to produce circular polarisation and increased bandwidth for cylindrical dielectric resonator antenna," *Electronics Letters*, Vol. 37, No. 7, 406–408, 2001.

[7] Hui, K. Y. and K. M. Luk, "Bandwidth enhancement of small dielectric resonator loaded patch antenna," *IEEE Transactions on Antennas and Propagation*, Vol. 54, No. 6, 1882–1885, 2006.

[8] Chang, T.-H. and J.-F. Kiang, "Broadband dielectric resonator antenna with an offset well," *IEEE Antennas and Wireless Propagation Letters*, Vol. 6, 564–567, 2007.

[9] Khamas, S. K., "Circularly polarized dielectric resonator antenna excited by a conformal wire," *IEEE Antennas and Wireless Propagation Letters*, Vol. 7, 240–242, 2008.

[10] Li, B., C.-X. Hao, and X.-Q. Sheng, "A dual-mode quadrature-fed wideband circularly polarized dielectric resonator antenna," *IEEE Antennas and Wireless Propagation Letters*, Vol. 8, 1036–1038, 2009.

[11] Sulaiman, M. I. and S. K. Khamas, "A singly fed rectangular dielectric resonator antenna with a wideband circular polarization," *IEEE Antennas and Wireless Propagation Letters*, Vol. 9, 615–618, 2010.

[12] Ortiz, N., F. Falcone, and M. Sorolla, "Enhanced gain dual band patch antenna based on complementary rectangular split-ring resonators," *Microwave and Optical Technology Letters*, Vol. 53, No. 3, 590–594, 2011.

[13] Pan, Y. M. and K. W. Leung, "Wideband omnidirectional circularly polarized dielectric resonator antenna with parasitic strips," *IEEE Transactions on Antennas and Propagation*, Vol. 60, No. 6, 2992–2997, 2012.

[14] Sahu, B., P. Tripathi, R. Singh, and S. P. Singh, "Dual segment rectangular dielectric resonator antenna with metamaterial for improvement of bandwidth and gain," *International Journal of RF and Microwave Computer-Aided Engineering*, Vol. 24, No. 6, 646–655, 2014.

[15] Pan, Y. M. and S. Y. Zheng, "A low-profile stacked dielectric resonator antenna with high-gain and wide bandwidth," *IEEE Antennas and Wireless Propagation Letters*, Vol. 15, 68–71, 2015.

[16] Chowdhury, R. and R. K. Chaudhary, "Wideband circularly polarized rectangular DRA fed with dual pair of right-angled microstrip line," *International Journal of RF and Microwave Computer-Aided Engineering*, Vol. 26, No. 8, 713–723, 2016.

[17] Gupta, A. and R. K. Gangwar, "Dual-band circularly polarized aperture coupled rectangular dielectric resonator antenna for wireless applications," *IEEE Access*, Vol. 6, 11 388–11 396, 2018.

[18] Altaf, A. and M. Seo, "Triple-band dual-sense circularly polarized hybrid dielectric resonator antenna," *Sensors*, Vol. 18, No. 11, 3899, 2018.

[19] Yang, M., Y. Pan, and W. Yang, "A singly fed wideband circularly polarized dielectric resonator antenna," *IEEE Antennas and Wireless Propagation Letters*, Vol. 17, No. 8, 1515–1518, 2018.

[20] Iqbal, J., U. Illahi, M. I. Sulaiman, M. M. Alam, M. M. Su'ud, M. N. M. Yasin, and M. H. Jamaluddin, "Bandwidth enhancement and generation of CP by using parasitic patch on rectangular DRA for wireless applications," *IEEE Access*, Vol. 7, 94 365–94 372, 2019.

[21] Illahi, U., J. Iqbal, M. I. Sulaiman, M. M. Alam, M. M. Su'ud, and M. H. Jamaluddin, "Singly-fed rectangular dielectric resonator antenna with a wide circular polarization bandwidth and beamwidth for WiMAX/Satellite applications," *IEEE Access*, Vol. 7, 66 206–66 214, 2019.

[22] Ballav, S. and S. K. Parui, "A wideband dielectric resonator antenna array using air-bridgeless coplanar waveguide power divider," *International Journal of RF and Microwave Computer-Aided Engineering*, Vol. 29, No. 9, e21858, 2019.

[23] Illahi, U., J. Iqbal, M. I. Sulaiman, M. Alam, M. M. Su'ud, and M. I. Khattak, "Design and development of a singly-fed circularly polarized rectangular dielectric resonator antenna for WiMAX/Satellite/5G NR band applications," *AEU — International Journal of Electronics and Communications*, Vol. 126, 153443, 2020.

[24] Gaya, A., M. H. Jamaluddin, I. Ali, and A. A. Althuwayb, "Circular patch fed rectangular dielectric resonator antenna with high gain and high efficiency for millimeter wave 5G small cell applications," *Sensors*, Vol. 21, No. 8, 2694, 2021.

[25] Zambak, M. F., M. N. M. Yasin, I. Adam, J. Iqbal, and M. N. Osman, "Higher-order-mode triple band circularly polarized rectangular dielectric resonator antenna," *Applied Sciences*, Vol. 11, No. 8, 3493, 2021.

[26] Illahi, U., J. Iqbal, M. Irfan, M. I. Sulaiman, M. A. Khan, A. Rauf, I. Bari, M. Abdullah, F. Muhammad, G. Nowakowski, and A. Glowacz, "A novel design and development of a strip-fed circularly polarized rectangular dielectric resonator antenna for 5G NR Sub-6 GHz band applications," *Sensors*, Vol. 22, No. 15, 5531, 2022.

[27] Ali, A., M. N. M. Yasin, I. Adam, A. H. Rambe, M. H. Jamaludin, H. A. Rahim, C. Cengiz, and M. I. S. A. Razak, "Triple-band circularly polarized dielectric resonator antenna (DRA) for wireless applications," *Computers, Materials & Continua*, Vol. 75, No. 1, 313–325, 2023.

[28] Chaitanya, B. and K. Manjunathachari, "Modified microstrip feed hybrid rectangular dielectric resonator antenna for wireless tri-band applications," *Measurement Science Review*, Vol. 23, No. 6, 281–287, 2023.

[29] Abdou, T. S. and S. K. Khamas, "A multiband millimeter-wave rectangular dielectric resonator antenna with omnidirectional radiation using a planar feed," *Micromachines*, Vol. 14, No. 9, 1774, 2023.

[30] Misala, S. and S. A. Mosa, "A novel stacked rectangular with surface mounted short rectangle dielectric resonator antenna in C-band applications," *Progress In Electromagnetics Research Letters*, Vol. 115, 81–89, 2024.

[31] Khan, S., O. Khan, K. Raheel, S. A. A. Shah, B. T. Malik, S. Khan, N. Gohar, and S. Koziel, "A highly compact split ring resonator-based rectangular dielectric resonator antenna with multiband characterization," *IEEE Access*, Vol. 13, 2360–2376, 2024.

[32] Vahora, A. and K. Pandya, "Triple band dielectric resonator antenna array using power divider network technique for GPS navigation/Bluetooth/Satellite applications," *International Journal of Microwave and Optical Technology*, Vol. 15, No. 4, 369–378, 2020.

[33] Vahora, A. and K. Pandya, "Implementation of cylindrical dielectric resonator antenna array for Wi-Fi/wireless LAN/Satellite applications," *Progress In Electromagnetics Research M*, Vol. 90, 157–166, 2020.